SciEn

Proceedings of 8th International Conference on Mechanical Engineering and Renewable Energy 2025
10-12 December, 2025, Chattogram, BANGLADESH

SciEn Conference Series: Engineering Vol. 4, 2026, pp 201-206 https://doi.org/10.38032/scse.2026.4.104

High-Performance Aluminium Hybrid Composited Reinforced with Zn, Sn and Ti for Lightweight Automotive and Advanced Structural Applications

Md. Shahriar Islam, Paban Barua Nishan, Pritom Barua Shuvo*

Department of Mechanical Engineering, Chittagong University of Engineering & Technology, Chattogram-4349, Bangladesh

ABSTRACT

This study focuses on the fabrication and characterization of high-performance aluminium hybrid metal matrix composites (AMMCs) reinforced with zinc (Zn), tin (Sn), and titanium (Ti) for lightweight automotive and advanced structural applications. Using the stir casting process, three hybrid composite formulations were developed by varying reinforcement ratios to optimize mechanical performance. Comprehensive tests, including tensile strength, Brinell hardness, and Charpy impact, were conducted, alongside scanning electron microscopy (SEM) and energy-dispersive spectroscopy (EDS) for microstructural analysis. The results revealed significant enhancements over pure aluminium, with the highest tensile strength of 292 MPa, maximum hardness of 67 BHN, and improved impact toughness of 2.4 J/cm². Microstructural observations confirmed uniform particle distribution in the optimally reinforced sample, contributing to superior mechanical properties. Owing to their high strength-to-weight ratio, these hybrid composites are highly suitable for engine blocks in automotive systems and aircraft seat frame structures, where weight reduction and structural integrity are critical. The outcomes demonstrate that combining Zn, Sn, and Ti reinforcements provides a synergistic enhancement in mechanical performance, offering a sustainable pathway for developing next-generation lightweight structural materials in automotive and aerospace engineering.

Keywords: Aluminium hybrid composites, Zn-Sn-Ti reinforcements, stir casting, lightweight design.

1. Introduction

The demand for lightweight, high-performance materials has grown significantly due to advancements in automotive, aerospace, and structural engineering applications, where reducing weight while improving strength and durability is critical. In automotive engineering, reducing vehicle weight by approximately 10% can lead to a 6%-8% improvement in fuel efficiency [1]. Similarly, in aerospace, the adoption of lightweight materials is pivotal for enhancing fuel efficiency and reducing emissions [2]. Among various engineering materials, metal matrix composites (MMCs) have garnered significant attention due to their superior mechanical, thermal, and wear properties compared to monolithic alloys. MMCs offer increased specific strength, stiffness, improved wear resistance, damping capabilities, good corrosion resistance, and low thermal expansion [3]. They consist of a metallic matrix reinforced with hard particles, fibers, or secondary phases to enhance strength, hardness, and thermal stability [4]. Among various MMCs, aluminium metal matrix composites (AMMCs) have received the most attention owing to aluminium's low density, high corrosion resistance, thermal stability, and excellent thermal conductivity. The addition of reinforcements is either ceramics, metals, or hybrid particles, offers substantial improvements in tensile strength, hardness, stiffness, and wear resistance [5]. Studies of Zn-reinforced Al matrices report that small amounts of Zn can significantly alter properties. For example, Agbeleye et al. cast recycled Al cans with 0–2 wt.% Zn particulates and found that the Zn particles dispersed and partly dissolved into the Al matrix [6]. At low Zn (≈1 wt.%), hardness initially decreased, but further Zn raised hardness. Ultimate tensile strength (UTS) grew with Zn up to ≈0.75 wt.% then fell (to about 97 MPa), while ductility, impact energy and corrosion resistance all improved with more Zn. In another work, Sonker et al. used powder metallurgy to fabricate Al–Zn/SiC composites and found that adding Zn (with SiC) increased tensile strength and hardness and greatly reduced wear loss compared to unreinforced Al [7]. Whereas, Tin is typically added to Al to impart self-lubricating and damping properties. Melt-spinning of Al–20 wt.%Zn alloys with 0–1.5 wt.% Sn (bearing alloys) revealed that Sn forms Sn–Zn intermetallics and strongly refines the microstructure [8] The alloy with 1.5 wt.% Sn had *finer grains* and the highest hardness/creep resistance among the series. This suggests Sn acts as a potent solid-solution or precipitation-strengthening element in Al. In another hybrid system, Farahany et al. added Sn (and Bi) to an A356–(Al_2O_3+ZrO_2+SiC) composite via compo-casting. SEM/EDS confirmed Sn/Bi segregation in interdendritic eutectic regions [9] Titanium, as a ductile metal reinforcement, is less common but growing in interest for its toughness benefits. K. K. Alaneme et al. noted that replacing ceramic reinforcements with ductile metals (e.g. Cu) in an Al–10Zn matrix yielded composites with much higher tensile strength and toughness [10]. Very few studies explore these elements in combination. The closest examples are binary or hybrid mixes. For instance, the rapid-solidification work on Al–Zn–Sn alloys [11] Zhang *et al.* [12] achieved refined grain microstructures and enhanced interfacial bonding by generating $TiAl_3$ intermetallics in situ via laser-based processing. Complementing these findings, Lei *et al.* [13] demonstrated that intrinsic heat treatment during wire-arc additive manufacturing of TiC/Ti reinforced Al–Zn–Mg–Cu resulted in superior hardness and tensile performance by mitigating microstructural heterogeneity. Collectively, these studies illustrate that coupling in-situ reinforcement strategies with advanced fabrication methods can unlock the true mechanical potential of AMCs.

In this study, Al-based hybrid composites reinforced with Zn, Sn, and Ti are fabricated using the bottom-pour stir casting technique. The primary objective is to investigate the influence of different Zn–Sn–Ti compositions on tensile strength, hardness, and impact energy while analyzing the microstructural uniformity using SEM and EDS techniques. The findings are expected to establish a new pathway for designing high-performance lightweight materials applicable in engine blocks, aircraft seat frames, and other advanced structural applications requiring superior mechanical integrity.

2. Materials And Methods

High-purity aluminium powder (99.9%) was selected as the base matrix material, with an average particle size below 100 µm to facilitate melting and uniform mixing. The reinforcements consisted of commercially available powders of zinc (99.5%), tin (99.5%), and titanium (99%), each prepared in fine form to ensure effective dispersion within the molten aluminium. Three different composite formulations were designed, maintaining aluminium as the primary constituent (~90 wt%) while varying the proportions of Zn, Sn, and Ti. The first composition contained 4 wt% Ti, 4 wt% Zn, and 2 wt% Sn, the second combined 2 wt% Ti, 4 wt% Zn, and 4 wt% Sn, and the third incorporated 2 wt% Ti, 6 wt% Zn, and 2 wt% Sn. These specific combinations were selected to investigate the influence of different reinforcement ratios on the mechanical and microstructural behavior of the aluminium matrix composites.

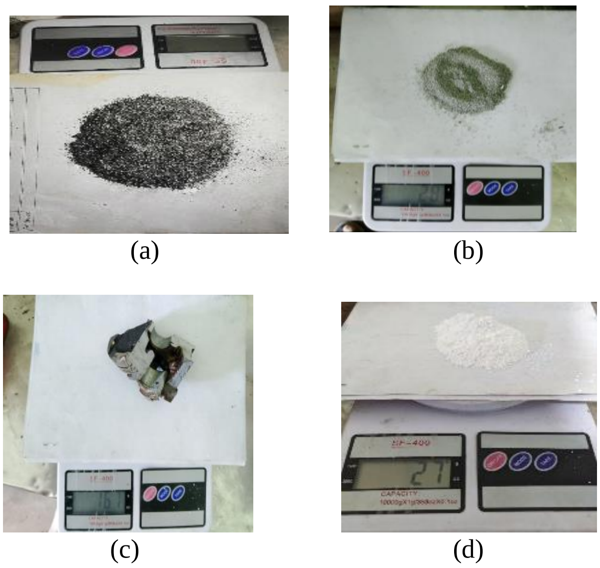

Fig. 1 (a) Aluminium Powder, (b) Zinc Powder, (c) Tin, (d) Titanium Powder.

2.1 Composite Fabrication via Stir Casting

Powdered constituents were first weighed to the prescribed ratios and then preheated to minimize oxidation. Aluminum, zinc, and tin powders were preheated at 400 °C for 1 hour, while titanium powder was preheated at 1000 °C for 1.5 hours. After preheating, each material was melted in a furnace: Al at ~660 °C, Zn at ~650 °C, Sn at ~232 °C, and Ti at ~1650 °C. Once the Al matrix had liquefied, a mechanical stirrer was inserted, generating a vortex at 100 rpm. The reinforcement powders (Ti, Zn, Sn) were then added gradually into the vortex. The melt was continuously stirred for approximately 5 minutes to achieve a homogeneous dispersion of the particles.

The uniform molten composite was then poured into preheated molds to solidify. Steel molds were fabricated with the required shapes for each specimen type (tensile, impact, and SEM samples). The cast metal was poured into these three molds and allowed to solidify. In total, eight samples covering the different compositions were produced by this stir-casting procedure.

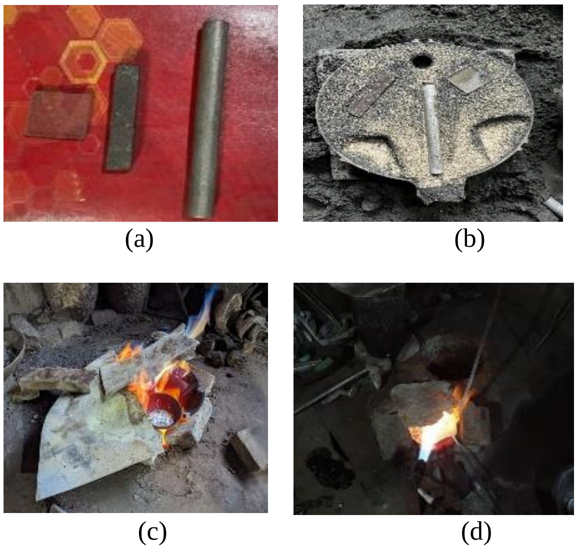

Fig. 2 (a) Patterns for making mold, (b) Mold, (c) Pouring Powder for Melting, (d) Stirring.

2.2 Specimen Machining and Shaping

After solidification, the cast billets were demolded and subjected to finishing operations. Turning and Threading: The cylindrical castings were machined on a lathe. Tensile specimens were turned to the final gauge diameter and length, and a threaded end was cut for gripping in the testing machine. Notching: Charpy impact specimens were machined with a U/V-shaped notch (slotting on a milling or slotter) to create a defined impact point. Grinding/Polishing: Finally, specimen faces and edges were ground and polished to ensure smooth, flat surfaces and precise dimensions. All final specimen geometries match the requirements for tensile (ASTM E8 dog-bone), impact (ASTM E23 V-notch), and Brinell hardness testing.

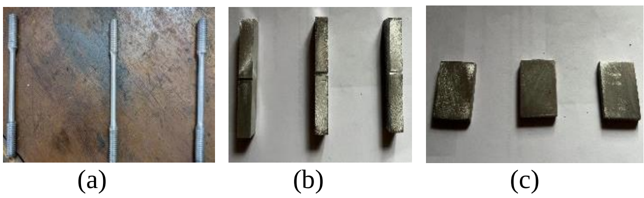

Fig. 3 (a) Final Specimen for Tensile Test, (b) Final Specimen for Impact Test, (c) Final Specimen for Hardness Test.

2.3 Mechanical Testing

- **Tensile Testing:** Quasi-static tensile tests were performed at room temperature using a Universal

Testing Machine (UTM). Cylindrical specimens (gauge diameter ~5 mm, gauge length ~50 mm) were loaded at a constant crosshead speed (per ASTM E8/E8M) until fracture. The load and extension were recorded, and ultimate tensile strength and ductility were calculated from the stress–strain curves. (The UTM used was the Universal Testing Machine of the CUET Solid Mechanics Laboratory, operated under displacement control.)

- **Impact Testing:** Charpy V-notch impact tests were conducted on a digital pendulum impact tester. U-notched specimens (2 mm depth notch) were broken by a swinging hammer, and the absorbed energy (in joules) was recorded directly by the instrument. Tests followed the ASTM E23 standard; each reading represents the average of at least three strikes.
- **Hardness Testing:** Brinell hardness measurements were carried out using a standard Brinell hardness tester. A 10 mm diameter hardened steel ball indenter was pressed into the specimen surface under a 3 kN (≈306 kgf) load for 30 seconds. The diameter of the resulting indentation was measured and used to calculate the Brinell Hardness Number (BHN) by the standard formula. Five readings were taken on each sample and averaged.

Fig. 4 (a) Universal Testing Machine (UTM), (b) Digital Impact Test Machine, (c) Brinell Hardness Testing Machine.

2.4 Microstructural and Elemental Analysis (SEM and EDS)

Fracture and polished cross-section surfaces of the composites were examined by scanning electron microscopy (SEM) to characterize the microstructure. SEM imaging was performed using a JEOL JCM-7000 (NeoScope) equipped with a secondary-electron detector (SED) under high vacuum at an accelerating voltage of 15 kV, a working distance of 13.4 mm, and at 2000× magnification (field of view ≈ 64 × 48 µm); scan time was 10 s. SEM provided high-resolution images of the aluminium matrix and the distribution of Ti, Zn, and Sn particles. In conjunction with SEM, energy-dispersive X-ray spectroscopy (EDS) was used to analyze the elemental composition of the composites. In the EDS analysis, the focused electron beam induces emission of characteristic X-rays from the sample; a detector measures the energy of these X-rays to quantify the relative concentrations of Al, Ti, Zn, and Sn in each region of the sample. These techniques confirmed the presence and uniform dispersion of the reinforcement elements within the aluminium matrix.

3. Results and Discussion

3.1 Tensile Strength

The three aluminum–Zn–Sn–Ti composites exhibited significantly different tensile strengths (UTS), reflecting their varying reinforcement compositions. Sample (iii) – with 90%Al + 6%Zn + 2%Ti + 2%Sn – achieved the highest UTS (≈292.151 MPa), markedly above Sample (i) (90%Al + 4%Ti + 4%Zn + 2%Sn, 239.926 MPa) and Sample (ii) (90%Al + 2%Ti + 4%Zn + 4%Sn, 260.461 MPa). This enhancement is attributed to the more uniform dispersion of hard particles in Sample (iii), as seen in SEM (see below), which promotes efficient load sharing. In contrast, Sample (i) – with higher Ti content but evident particle clustering – showed the lowest strength. The data indicate that reducing Sn from 4% to 2% while raising Zn to 6% (Sample iii) significantly increases tensile strength. Compositions with Zn below 6% or higher Sn (as in Samples i and ii) suffered from reinforcement segregation during solidification, leading to lower tensile performance. Thus, the balance of Zn and Sn is critical: the Zn-rich, Sn-reduced alloy (Sample iii) maximized UTS, whereas higher Sn or inadequate Zn content reduced it.

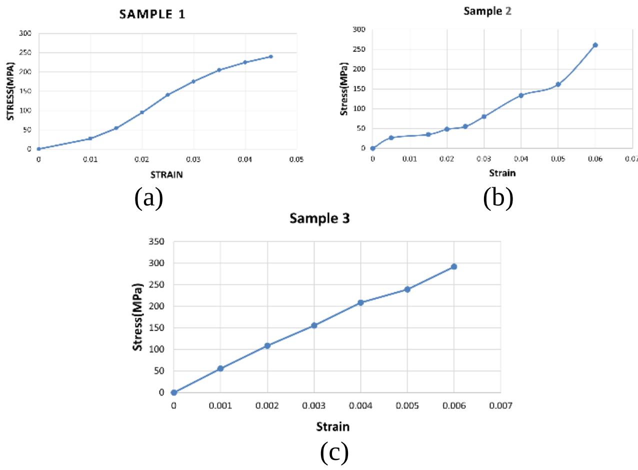

Fig. 5 (a) Stress versus strain graph for Sample 1, (b) Stress versus strain graph for Sample 2, (c) Stress versus Strain curve for Sample 3.

3.2 Hardness Behavior

Brinell hardness testing showed a similar dependence on composition. Sample (i) (4%Ti, 4%Zn, 2%Sn) exhibited the highest hardness (≈67.25 BHN), whereas Sample (ii) (2%Ti, 4%Zn, 4%Sn) was softest (≈55.38 BHN); Sample (iii) (2%Ti, 6%Zn, 2%Sn) was intermediate (≈61.50 BHN). In effect, increasing the Sn content (from 2% to 4%, Sample ii) while reducing Ti greatly lowered hardness, and restoring a 2%Sn level (Sample iii) recovered hardness somewhat. This suggests that Ti provides a stronger hardening effect than Sn in these composites. The highest Ti-bearing sample (Sample i) was the hardest, whereas replacing Ti with more Sn (Sample ii) yielded the softest composite. The partial hardness gain in Sample (iii) (with more Zn) indicates Zn contributes moderate reinforcement. Overall, the hardness trend mirrors the reinforcement mix: the Ti-rich alloy is hardest, the Sn-rich alloy is softest, and the Zn-rich alloy lies between.

3.3 Impact Energy Absorption

Impact testing revealed that Sample (ii) (4%Sn, 4%Zn, 2%Ti) absorbed the most energy: about 1.9 J and an impact strength of ≈2.4 J/cm². Sample (i) and Sample (iii) both absorbed ≈1.7 J, but with lower impact strengths (≈1.8 and 2.1 J/cm², respectively). In other words, the Sn-rich composite (Sample ii) was toughest.

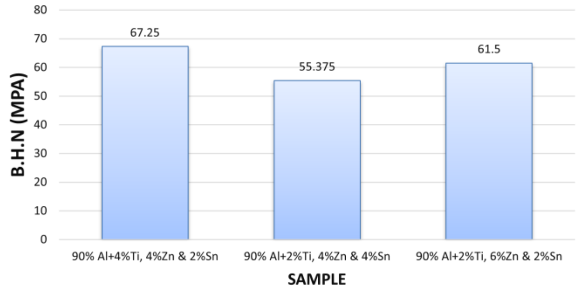

Fig. 6 Brinell Hardness Number of Composites.

The data imply that increasing Sn content significantly improves toughness: raising Sn from 2% (Sample i) to 4% (Sample ii) (while reducing Ti) increased impact strength by ~33%. Conversely, increasing Zn from 4% to 6% (Sample iii vs. Sample ii) gave only a modest strength increase. These results indicate the Sn/Ti ratio strongly affects impact behavior. In brief, the sample with balanced Ti, Zn, and higher Sn best dissipated impact energy, whereas samples with lower Sn (and/or higher Ti) showed reduced energy absorption. This composition-dependent trend is consistent with the SEM/EDS observations: the sample (ii) microstructure that combined moderate Ti with elevated Zn and Sn produced the highest impact strength.

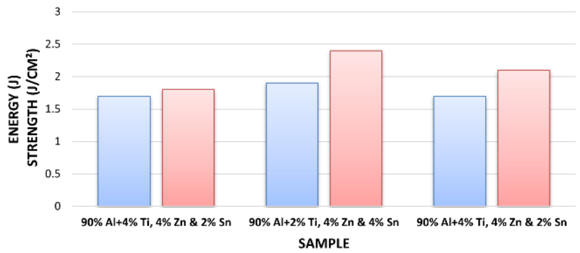

Fig. 7 Energy absorbed and strength comparison.

3.4 Microstructural Characterization

3.4.1 Morphological Characterization via SEM

SEM analysis elucidated the reinforcement morphology underlying these mechanical trends. Samples (i) and (ii) both exhibited irregular, angular reinforcement particles and clear local clustering. For Sample (i), the micrographs show numerous facets and sharp particles concentrated in pockets (non-uniform dispersion). Sample (ii) similarly displayed uneven distribution – some particles even appeared elongated or needle-like – with visible agglomerates in the matrix. By contrast, Sample (iii) showed a much more homogeneous structure: its particles were more rounded and evenly dispersed throughout the Al matrix with minimal clustering. This stark difference (uniform in Sample iii vs. clustered in Samples i and ii) explains why Sample iii achieved superior tensile strength and intermediate hardness.

3.4.2 Elemental Composition and Phase Identification

EDS spectra confirmed that all intended elements were present, though with some deviation from nominal ratios due to processing. For example, Sample (i) (target 90%Al+4%Ti+4%Zn+2%Sn) actually measured only ~88% Al with 5–6.7% Ti, 4–5% Zn and ~0.5% Sn. Sample (ii) (90%Al+4%Zn+4%Sn+2%Ti) showed roughly 91–92% Al, 6–7% Zn, 0.7–5% Ti and 1–2% Sn. Sample (iii) (90%Al+6%Zn+2%Sn+2%Ti) yielded ~92–93% Al, ~6% Zn, ~0.4% Ti and ~1% Sn.

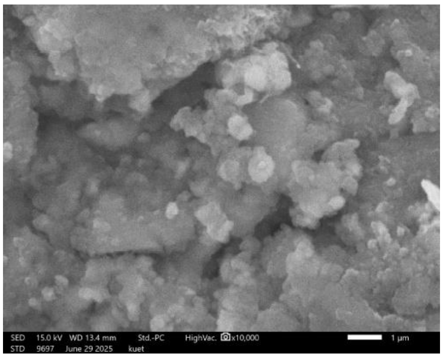

Fig. 8 SEM micrograph of sample (i) at 10k magnification.

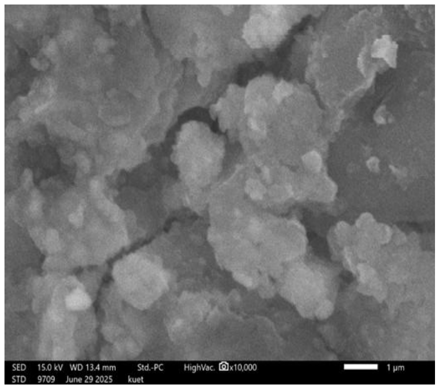

Fig. 9 SEM micrograph of sample (ii) at 10k magnification.

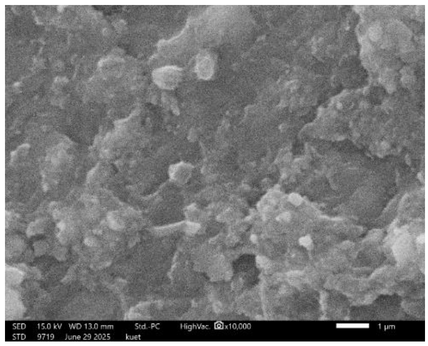

Fig. 10 SEM micrograph of sample (iii) at 10k magnification.

These deviations – consistently lower Sn and slightly shifted Al content – are attributed to incomplete stirring and particle segregation during casting. The EDS deviations arise from elemental segregation, oxidation, and partial volatilization during high-temperature casting. Titanium forms intermetallic like Al_3Ti, reducing its detectable amount, while Zn and Sn may oxidize or segregate. Moreover, EDS gives localized, not bulk, composition—causing inherent variation in multiphase composites. In summary, the micrographs and EDS together reveal that the superior properties of Sample (iii) arise from its well-dispersed reinforcements, whereas the more clustered morphologies and uneven compositions in Samples (i) and (ii) correlate with their relatively lower tensile and impact performance.

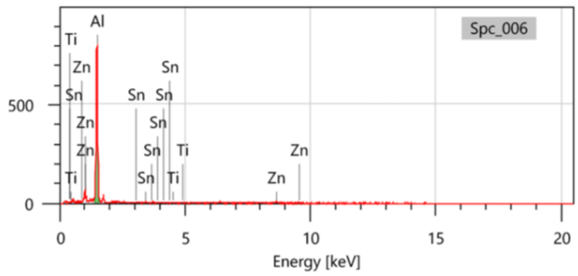

Element	Atom%
Al	84.91±3.56
Ti	8.81±4.62
Zn	6.05±2.38
Sn	0.24±0.17
Total	100.00
Spc_006	Fitting ratio 0.1216

Fig. 11 EDS result of Al-90%, Zn-4%, Ti-4% & Sn-2%.

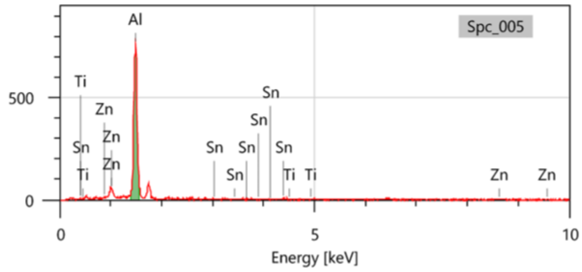

Al	91.12±3.89
Ti	0.74±5.58
Zn	7.07±1.28
Sn	1.07±0.92
Total	100.00
Spc_005	

Fig. 12 EDS result of Al-90%, Zn-4%, Sn-4% & Ti-2%

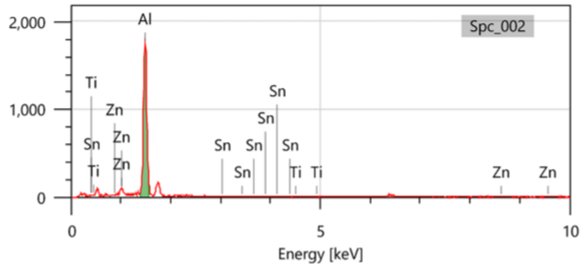

Al	92.78±2.61
Ti	0.03±0.18
Zn	6.79±3.08
Sn	0.41±0.47
Total	100.00
Spc_002	

Fig. 13 EDS result of Al-90%, Zn-6%, Sn-2% & Ti-2%.

3.5 Grain Size Distribution

SEM-based analysis confirmed that all three Al–Ti–Zn–Sn composites exhibited mixed grain populations, with histograms showing near-normal distributions of both fine and coarse grains. Samples 1 (4%Ti–4%Zn–2%Sn) and 2 (2%Ti–4%Zn–4%Sn) contained more irregular and angular grains with localized clustering, indicating heterogeneous growth. In contrast, Sample 3 (2%Ti–6%Zn–2%Sn) displayed a finer and more equiaxed morphology, with reinforcement particles distributed more uniformly across the matrix. These results demonstrate that higher Zn content promoted grain refinement and homogeneity, while increased Ti or Sn content tended to produce coarser and less uniform structures. Grain size was quantified using ImageJ and Origin software following the ASTM E112 line-intercept method. ImageJ extracted grain diameters from calibrated SEM images, and Origin plotted their distribution histograms. This confirmed microstructural refinement and uniform grain dispersion among compositions.

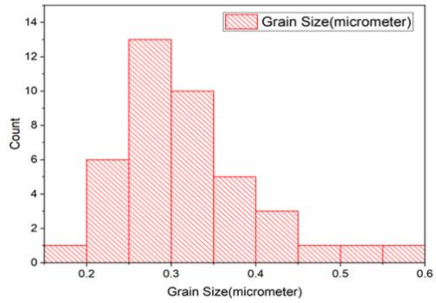

(i)

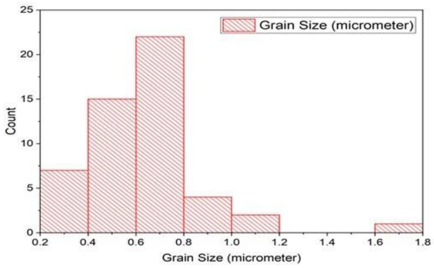

(ii)

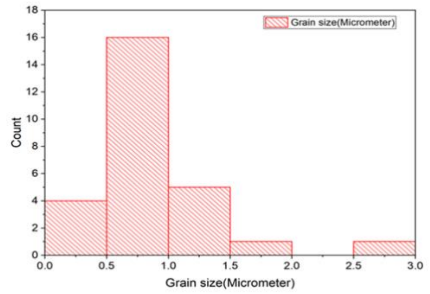

(iii)

Fig. 14 Normal distribution curve analysis of sample (i), (ii), (iii).

3.6 Summary Results

Table 1 Summary of the Results.

Sample	**90% Al+ 4% Zn + 2% Sn +4% Ti**	**90% Al+ 4% Zn+ 4% Sn+ 2% Ti**	**90% Al+ 6%Zn + 2% Ti+ 2% Sn**
Impact Strength (J/cm^2)	1.8	2.4	2.1
Tensile Strength (MPa)	239.926	260.461	292.151
Hardness (BHN)	67.25	55.375	61.5

4. Conclusion

The experimental program produced three Al–Zn–Sn–Ti hybrid composites via stir casting and demonstrated clear, composition-dependent property trade-offs: When compared with the unreinforced aluminum baseline, all hybrid composites displayed pronounced improvements, with tensile strength increasing by over 150%, hardness by nearly 140%, and impact toughness by about 160%. This validates the positive reinforcement synergy of Zn, Sn, and Ti in the Al matrix. the Zn-rich alloy (Sample III: 90Al–6Zn–2Ti–2Sn) delivered the highest ultimate tensile strength (~292 MPa), the Ti-enriched variant (Sample I: 90Al–4Ti–4Zn–2Sn) showed the greatest hardness (~67 BHN), and the Sn-boosted composition (Sample II: 90Al–2Ti–4Zn–4Sn) provided the best impact resistance (~2.4 J/cm²). Microstructural inspection linked these outcomes to particle distribution and grain form — Sample III exhibited the most uniform dispersion and finer, equiaxed grains, while Samples I and II displayed localized clustering and more irregular morphologies — and EDS mapping indicated local departures from nominal chemistry consistent with incomplete mixing. Taken together, the measured property set and microstructure suggest these cast hybrids have promise for weight-sensitive structural components such as automotive body panels and engine blocks/heads, and for aerospace structural elements (e.g., seat frames) where tailored combinations of strength, hardness and toughness are required. To unlock their full potential, process refinements (enhanced stirring protocols, optimized feed sequence and post-cast homogenization) are recommended to minimize segregation and improve reproducibility.

5. References

[1] Cheah, L.W., 2010. 2010. Cars on a diet: the material and energy impacts of passenger vehicle weight reduction in the US (Doctoral dissertation, Massachusetts “Lightweight Materials for Cars and Trucks Institute of Technology).

[2] Singh, J., Srivastawa, K., Jana, S. and Dixit, C., 2024. Advancements in lightweight materials for aerospace structures: A comprehensive review. *Acceleron Aerospace Journal*, *2*(3), pp.173-183.

[3] Pooja, K., Tarannum, N. and Chaudhary, P., 2025. Metal matrix composites: revolutionary materials for shaping the future. *Discover Materials*, *5*(1), p.35.

[4] Gupta, P.K., Trivedi, A.K., Gupta, M.K. and Dixit, M., 2024. Metal matrix composites for sustainable products: A review on current development. *Proceedings of the Institution of Mechanical Engineers, Part L: Journal of Materials: Design and Applications*, *238*(10), pp.1827-1864.

[5] Samal, P., Vundavilli, P.R., Meher, A. and Mahapatra, M.M., 2020. Recent progress in aluminum metal matrix composites: A review on processing, mechanical and wear properties. *Journal of Manufacturing Processes*, *59*, pp.131-152.

[6] Agbeleye, A., Durowaye, S., Oladoye, A. and Bolasodun, B., 2021. Effect of Zinc Addition on the Mechanical and Corrosion Characteristics of Aluminium Matrix Composites. *Acta Materialia Turcica*, *5*(1), pp.30-37.

[7] Sonker, P.K., Singh, T.J. and Yadav, N.P., 2023. Experimental research and effect on mechanical and wear properties of aluminium based composites reinforced with Zn/Sic particles. *Discover Materials*, *3*(1), p.9.

[8] Abdelhakim, N.A. and Shalaby, R.M., 2021. Microstructures and mechanical properties of Al-Zn-Sn bearing alloys for high performance applications. *World Journal of Engineering and Technology*, *9*(3), pp.637-652.

[9] Farahany, S., Hamdani, M.K., Salehloo, M.R., Krol, M. and Cheraghali, E., 2024. Synthesis and Characterization of Novel Aluminum Composites: A Compo-Casting Approach with ZrO2, Al2O3, and SiC. *Archives of Foundry Engineering*, pp.88-97.

[10] Alaneme, K.K., Ojomo, A.M. and Bodunrin, M.O., 2022. Structural analysis, mechanical and damping behaviour of Al-Zn based composites reinforced with Cu and SiC particles. *Manufacturing Review*, *9*, p.5.

[11] Sonker, P.K., Singh, T.J. and Yadav, N.P., 2023. Experimental research and effect on mechanical and wear properties of aluminium based composites reinforced with Zn/Sic particles. *Discover Materials*, *3*(1), p.9.

[12] Tian, C., Singh, K., Wakai, A., Dass, A., Bustillos, J., Chuang, A.C. and Moridi, A., 2025. Tunable TiAl3-reinforced aluminum matrix composites via in-situ reactive printing: insights from operando synchrotron analysis and microstructural characterization. *npj Advanced Manufacturing*, *2*(1), p.3.

[13] Lei, D., Xu, S., Yang, X., Lu, X., Qin, X., Zhou, L., Chen, J. and Li, M.V., 2025. Transformation mechanism of microstructure and mechanical properties of wire arc additive manufacturing TiC/Ti reinforced Al-Zn-Mg-Cu alloy under different heat treatment processes. *Journal of Alloys and Compounds*, p.180718.